The International Archives of the Photogrammetry, Remote Sensing and Spatial Information Sciences, Volume XLVI-3/W1-2022
7th Intl. Conference on Ubiquitous Positioning, Indoor Navigation and Location-Based Services (UPINLBS 2022), 18–19 March 2022, Wuhan, China

VEHICLE POSITIONING IN UNDERGROUND SPACE USING A SMART PHONE

Leilei Li [1], Qihai Huang [1], Keyi Xu [1], Guangyi Guo [2], Ruizhi Chen [2]

[1] College of Aerospace Engineering, Chongqing University, China - lill@cqu.edu.cn, qhaihuang@foxmail.com, xukeyi_cqu@163.com

[2] State Key Laboratory of Information Engineering in Surveying, Mapping and Remote Sensing, Wuhan University, China - guangyi.guo@whu.edu.cn, chen@whu.edu.cn

Commission IV, WG IV/5

KEY WORDS: Underground Navigation, INS, Bluetooth, Non-Holonomic Constraint (NHC)

ABSTRACT:

Smartphones is a good choice for vehicle navigation since many navigation sensors are built-in with low cost advantage. However, it cannot provide reliable positioning information in underground space since GNSS is not available and IMU drift quickly. In this manuscript, a mixed navigation scheme for smartphone consumer is presented. It combines GNSS, INS, Non-Holonomic Constraint (NHC) and Bluetooth Low Energy (BLE) to provide reliable seamless navigation in both outdoors and underground. Some important problems including smartphone boresight misalignment, HNC level arm, GNSS and BLE time lag are discussed in the manuscript. The testing results show 3.1% /D horizontal positioning error in tunnel in INS/NHC positioning mode, and approximately 1 meter accuracy in underground parking garage in INS/NHC/BLE mode.

1. INTRODUCTION

High precision navigation does not being demanded as much as present because automated driving technologies is evolving at a rapid pace. It normally integrates GNSS RTK and other sensors, such as IMU, odometer, LiDar, camera, millimeter radar etc., to navigate in both outdoors and underground space. However, highly cost is the primary hurdle for these technologies being applied in consumer market.

In daily life, consumers are accustomed to use their smartphones to navigate, in which radio and motion sensors are built in, including GNSS, accelerometer, gyroscope, magnetometer, Bluetooth, Wi-Fi, etc. Though cheap sensors are built in the smartphone, it can achieve surprisingly performance after delicate calibration. For example, RTK positioning with the smartphone-quality data is applicable by latest innovations though poor antenna quality is used, which can be overcome by antenna calibration or coupling to the phone’s inertial sensors. However, low-cost mass-market navigation scheme in underground space is still challenging since inertial navigation has rapid degradation without GNSS.

To constrain INS in tunnel and underground parking garage, radio positioning method is normally used, such as Wi-Fi and Bluetooth based on AOA, TOA or fingerprint map. It requires pre-constructed navigation infrastructure. On the other hand, NHC is also can used as the virtual measurement for the integration with INS. It refers the premise that the lateral velocity and vertical velocity of the vehicle are zeros. The benefit resides in it is autonomous and infrastructure-free. However, the boresight and location of smartphone do not satisfy NHC premise at most of time. Consumers have different habits to place their smartphones, and probably different for every time of driving. It leads to phone frame and vehicle frame are un-aligned. Therefore, inertial motion detected by smartphone need to be transformed to vehicle frame to implement inertial navigation mechanization and NHC constraint. In addition, the smartphone is often located on the dash board while NHC condition only holds on the centre of back wheels. The location deviation will cause level arm effect when the vehicle makes turning. Therefore, the boresight misalignment and level arm between the smartphone and the vehicle must be calibrated before being used to constrain INS. And they cannot be calibrated in advance like factory-installed navigator since they depend on consumers and their choice every driving.

In this manuscript, a mixed navigation scheme for smartphone consumer is discussed. It combines GNSS/INS/NHC/Bluetooth to provide reliable seamless navigation in both outdoors and underground space. The calibration and constraint model for smartphone boresight misalignment and HNC level arm are built. To make quick and accurate convergence with large misalign angles, parallel filtering method with four reduced states filters are proposed to estimate the proper orientation of the phone. The INS/Bluetooth integration is also modelled with Bluetooth time lag augmented as state of filter. The testing results show 3.1% /D horizontal positioning error in tunnel in INS/NHC positioning mode, and correct route in underground parking garage in INS/NHC/BLE mode.

2. OVERRALL SCHEME OF THE SMART PHONE NAVIGATION

In the smartphone based mixed navigation scheme (shown in Figure 1), GNSS and INS are used to acquire the integrated solution in outdoors, meanwhile phone boresight misalignment and NHC level arm are evaluated by the filter online. When the vehicle runs in urban canyon, tunnel, and underground parking garage, NHC or ZUPT with calibrated boresight and level arm are used as virtual measurement to restrain INS error growing. If radio positioning infrastructure like BLE is available in underground space, it combines with INS/NHC to obtain the reliable solution.

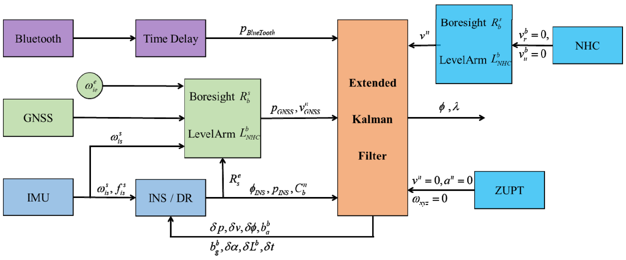

Figure 1. Mixed navigation scheme for smartphone consumer.

Extended Kalman Filter with states of navigation error, sensor error, NHC error and synchronization error was built as shown in Equation (1), where each kind of error state was listed in four lines. The navigation error includes attitude misalignment, velocity error and position error. Gyro bias and accelerometer bias are taking into account as sensor error, while scale factor is not accounted for calculation reason. NHC error includes smartphone boresight misalignment and NHC level arm. Synchronization error is often ignored in many navigation systems. Mixed navigation scheme requires time synchronized between multi-sensors. It often employs PPS of GNSS as time reference in a customized navigator. However, this mechanism is not implemented in smartphone. In fact, obvious time lag was observed in GNSS data and BLE data in a smartphone, and it changes with time. Therefore, GNSS time lag and BLE time lag are considered as synchronization error of EKF. GNSS level arm is not included because the antenna locates near the IMU in the smartphone.

$$x = \begin{bmatrix} (\phi)^T & (\delta v^n)^T & (\delta p)^T & \cdots \\ (\varepsilon^b)^T & (\nabla^b)^T & \cdots & \\ (\delta\alpha^b)^T & (\delta L_{nhc}^b)^T & \cdots & \\ \delta t_{gnss} & \delta t_{ble} & & \end{bmatrix}^T \tag{1}$$

where $\varphi =$ vehicle attitude misalignment angles
$\delta v^n =$ velocity errors
$\delta p =$ latitude, longitude and altitude errors, respectively
$\boldsymbol{\varepsilon}^b =$ gyro drift errors expressed in body frame
$\nabla^b =$ accelerometer biases errors expressed in body frame
$\alpha =$ boresight misalignment between smartphone and vehicle
$L_{nhc}^b =$ NHC lever arm
$\delta t_{gnss} =$ GNSS time lag error
$\delta t_{ble} =$ BLE time lag error

The differential state equations in navigation frame are shown in Equation (2-4). Sensor error is modelled as first-order Markov process as in Equation (5-6). GNSS time lag is also model as first-order Markov process as in Equation (7).

$$\dot{\varphi} = M_{aa}\varphi + M_{av}\delta v^n + M_{ap}\delta p - C_b^n \varepsilon^b \,, \tag{2}$$

$$\delta\dot{v}^n = M_{va}\varphi + M_{vv}\delta v^n + M_{vp}\delta p + C_b^n \nabla^b \,, \tag{3}$$

$$\delta\dot{p} = M_{pv}\delta v^n + M_{pp}\delta p \,, \tag{4}$$

$$\dot{\varepsilon}^b = -\beta_{\omega}\varepsilon^b + \xi_{\omega} \,, \tag{5}$$

$$\dot{\nabla}^b = -\beta_f \nabla^b + \xi_f \,, \tag{6}$$

$$\delta\dot{t}_{gnss} = -\beta_{gnss}\delta t + \xi_{gnss} \,, \tag{7}$$

where $M =$ state transition matrix of states
$\beta =$ time constant of Markov process
$\xi =$ Gaussian white noise

The measurements of the EKF are GNSS position, GNSS velocity, NHC velocity and BLE positioning. When GNSS is available, the measurement equations of EKF could be written as Equation (8-10), where GNSS velocity and position are used to integrate with INS.

$$Z = \begin{bmatrix} \tilde{v}_{ins}^n - v_{gnss}^n \\ \tilde{p}_{ins} + M_{pv}\tilde{v}_{ins}^n \Delta t_{gnss} - p_{gnss} \end{bmatrix} = HX + V \,, \tag{8}$$

$$H = \begin{bmatrix} 0_{3\times3} & I_{3\times3} & 0_{3\times3} & 0_{3\times12} & 0 & 0 \\ 0_{3\times3} & 0_{3\times3} & I_{3\times3} & 0_{3\times12} & M_{pv}\tilde{v}_{ins}^n & 0 \end{bmatrix}, \tag{9}$$

$$V = \begin{bmatrix} V_v \\ V_p \end{bmatrix}, \tag{10}$$

where $(\tilde{v}_E^n, \tilde{v}_N^n)_{ins} =$ east and north velocity estimated by INS
$(v_E^n, v_N^n)_{gnss} =$ east and north velocity estimated by GNSS
$\tilde{p}_{ins} =$ INS position
$p_{gnss} =$ GNSS position
$\Delta t_{gnss} =$ GNSS time lag
$V_v, V_p =$ velocity and position measurement noise.

In fact, most low cost GNSS modules do not output the velocity in navigation frame, instead by the forward speed of the vehicle. It can be combined with zero velocity measurements of NHC in lateral and vertical directions to form a full tri-axis constraint. It is worth noting that a corrected term caused by time lag is applied to GNSS position measurement as shown in Equation (8). The NHC measurement model will be discussed in the section 3 and section 4, respectively.

3. NHC CALIBRATION MECHNISAM

NHC refer to the fact that the velocity of the vehicle in the vertical plane perpendicular to the forward direction (Y-axis) is almost zero if there is no jump off or slides happen (Wang, 2020). It is valuable information to improve the navigation accuracy of GNSS/INS integration on interruption of GNSS signal, especially to the low-cost sensors. There are two critical factors, i.e., the boresight misalignment between vehicle and smartphone and lever arm from the smartphone to NHC point. It is necessary to calibrate and compensate them when NHC is applied in vehicle navigation. According to the vehicle steering theorem, when the vehicle turns, the front wheels control the direction, and the rear wheels do not deflect, as shown in Figure 2. Therefore, NHC condition is not meet on the whole vehicle. We can approximately consider NHC point locating at the rear wheel centre of vehicle.

Before start the derivation of NHC level arm and boresight misalignment, several frames are described in the following. The INS mechanism is implemented in navigation. The tri-axis of vehicle frame (v-frame) is defined by right, forward and up directions, corresponding to pitch, roll, and heading of the vehicle, as shown in Figure 3. The smartphone/sensor frame (s-frame) has similar definition. It is normally fixed by a mobile phone support near the dash board, which results in level arm to NHC center and boresight misalignment α, including pitch α_p, roll α_r and heading α_y. The level arm and relative orientation between smartphone and the vehicle can be modeled as a random constant since in most cases the mobile phone support is fixed.

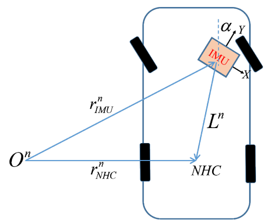

Figure 2. NHC level arm and boresight misalignment of smartphone

Figure 3. The vehicle frame and smartphone frame

Assuming the centre of turning circle is O^n and it is on the extension of the rear wheels' connection, as shown in Figure 2. The relationship between the three vectors is

$$r^n_{imu} = r^n_{nhc} - L^n , \tag{11}$$

where r^n_{imu} = coordinates vectors of IMU
r^n_{nhc} = coordinates vectors of NHC
L^n = the level arm between s-frame and NHC in n-frame

Appling the derivation to Equation (15) leads to:

$$\dot{r}^n_{imu} = \dot{r}^n_{nhc} - \dot{L}^n , \tag{12}$$

Then, the level arm vector can be transformed from the n-frame to the v-frame because it is usually measured and represented in the latter. Coriolis Law is also applied in the transformation. Given that level arm is a constant value, that is $\dot{L}^b = 0$, Equation (13) can be simplified as:

$$\dot{r}^n_{imu} = \dot{r}^n_{nhc} - C^n_v \Omega^v_{nv} L^v , \tag{13}$$

where C^n_v = transform matrix from v-frame to n-frame
Ω^b_{nb} = the skew symmetric matrix of angular rate of b-frame respect to n-frame represented in b-frame. It can be decomposed as:

$$\Omega^v_{nv} = \Omega^v_{sv} + \Omega^v_{is} - \Omega^v_{ie} - \Omega^v_{en} , \tag{14}$$

where Ω^v_{nv}, Ω^v_{sv}, Ω^v_{is}, Ω^v_{ie} and Ω^v_{en} = skew symmetric matrix of angular rate ω^v_{nv}, ω^v_{sv}, ω^v_{is}, ω^v_{ie} and ω^v_{en}, respectively. Considering v-frame have no relative angular movement respect to s-frame, that is $\Omega^v_{sv} = \left[0_{3\times3}\right]$, then Equation (15) can be simplified as:

$$\dot{r}^n_{imu} = \dot{r}^n_{nhc} - C^n_b \left(\Omega^b_{is} - \Omega^b_{ie} - \Omega^b_{en}\right) L^b , \tag{15}$$

As discussed in Section 2, GNSS module in smartphone outputs the forward speed in v-frame. Assuming there is no slides happened and ignoring level arm effect, then the GNSS speed v_{gnss} only corresponds to the forward direction of the vehicle. Therefore, the velocities of NHC and GNSS can be connected as:

$$v^v_{nhc} = C^v_n \dot{r}^n_{nhc} = \begin{bmatrix} 0 & v_{gnss} & 0 \end{bmatrix}^T , \tag{16}$$

Appling Equation (14) to Equation (13), it leads to:

$$v^v_{nhc} = C^v_n v^n_{imu} + (C^v_s \Omega^s_{is} C^s_v - C^v_n C^n_e \Omega^e_{ie} C^e_n C^n_v - C^v_n \Omega^n_{en} C^n_v) L^b . \tag{17}$$

where $C^v_n v^n_{imu}$ = INS velocity in v-frame
Presumed that C^n_v is the real direction cosine matrix from v-frame to n-frame and $\tilde{C}^n_v$ is the calculated matrix. The relationship between C^n_v and $\tilde{C}^n_v$ can be represented as:

$$C^n_v = \left(I + \phi \times\right) \tilde{C}^n_v , \tag{18}$$

where ϕ = attitude misalignment angle.
Similarly, the transformation caused by smartphone boresight misalignment α can be represented as:

$$C^s_v = C^s_{s'} C^{s'}_v = (I + \delta\alpha \times) \tilde{C}^s_v , \tag{19}$$

where $\delta\alpha$ = boresight misalignment error.
Expanding Equation (18) and omitting the second and high-order item, we obtain the measurement equations that can be constructed as:

$$Z = HX + v , \tag{20}$$

$$Z = v^v_{nhc} - \tilde{C}^v_n \tilde{v}^n_{imu} - \left[\tilde{C}^v_s \Omega^s_{is} \tilde{C}^s_v - C^v_e \Omega^e_{ie} c^e_v - \tilde{C}^v_n \Omega^n_{en} \tilde{C}^n_v\right] \tilde{L}^v , \tag{21}$$

$$H = \begin{bmatrix} h_\phi & h_v & 0_{3\times9} & h_\alpha & h_L & 0_{3\times2} \end{bmatrix} , \tag{22}$$

where δv^n_{imu} = IMU velocity error
h = observation matrix of EKF states.

4. BLE POSITIONING AND INTEGRATION WITH INS

BLE devices broadcast their ID messages to the portable electronic equipments (Hiromune, 2021). This technology allows smartphones, tablets and other devices to communicate in close to a beacon. Bluetooth beacons can transmit the universally unique identifiers received by compatible applications or operating systems when BLE devices close to them (Cao, 2019). The physical location of the device can be determined by the identifier and several bytes of information. And location-based operation on the client or trigger device can be monitored. The difference between Bluetooth beacons and other location-based technologies is that broadcast devices can

simply transmit signals to the receiving device but it is required to install some specific application on the receiving devices to interact with the beacon.
Bluetooth low-energy pseudolite station can be used to assist vehicle navigation. These stations consist of BLE chips, which are combined with UKF-based positioning engine and navigation messages. Users can use ordinary smart phones to receive navigation messages which in the form of broadcast, and it can achieve accurate positioning (Hiromune, 2021).
The BLE pseudolite module includes multiple Bluetooth chips and a microcontroller (MCU). MCU is the control center of each chip and multiple Bluetooth chips are used to overcome the instability of a single Bluetooth chip signal. In order to minimize the mutual interference between chips, Bluetooth chips are evenly distributed on the edge of the circular module.
Angle of arrival (AOA) measurement is that the transmitter sends special data packets through a single antenna, and the receiver receives them through multiple antennas. Phase is different because the distances from each antenna to the transmitter are different. Angle relationship between antennas can be calculated by phase difference and distance between antennas, and direction can be found by trilateration method.

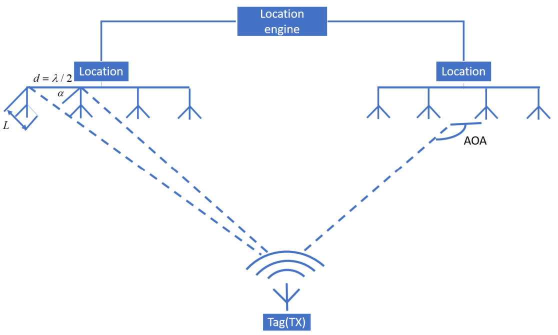

Figure 4. Bluetooth positioning diagram

When the BLE pseudolite works, the Bluetooth chip sends the navigation messages in the form of broadcast. The distance between each BLE pseudolite and the positioning device can be calculated by the following distance formula:

$$d = 10^{(abs(RSSI)-A)/(10\times n)}, \tag{23}$$

Where d is the distance between BLE pseudolite and the positioning device, RSSI represents the received signal strength, A is the strength of signal value when the transmitter and receiver are 1m away, and n is the environmental attenuation factor.
Smartphone sensors will send a set of speed, navigation information, BLE pseudolite distance and previous positioning results as parameters to UKF during positioning. UKF localization algorithm includes initialization and calculation. The calculation includes the following three steps: first, calculating sigma points, then update prediction, and finally update measurement values.
When vehicle drive in underground parking garage, the measurements of the EKF is BLE positioning. The measurement equations of EKF could be written as Equation (24-26).

$$Z = \left[\tilde{p}_{ins} + M_{pv}\tilde{v}^n_{ins}\Delta t_{ble} - p_{ble}\right] = HX + V, \tag{24}$$

$$H = \begin{bmatrix} 0_{3\times3} & 0_{3\times3} & I_{3\times3} & 0_{3\times12} & 0 & M_{pv}\tilde{v}^n_{ins} \end{bmatrix}, \tag{25}$$

$$V = \left[V_p\right], \tag{26}$$

where $\tilde{p}_{ins}$ = INS position
p_{ble} = BLE position
Δt_{ble} = BLE time lag
V_p = position measurement noise.

5. REDUCED PARALLEL FILTERS FOR NHC CALIBRATION

Equation (16-18) are the observation model of INS/NHC integration. The smartphone boresight misalignment and NHC level arm can be calibrated outdoor and constrain INS indoor. However, the derivation is based on the premise that the misalignment is small angles. The smartphone does not have a fixed location and orientation every driving; therefore, the initial boresight misalignment cannot be pre-calibrated as factory setting. If orientation is wrongly initialized, the filter will run with divergence. In addition, IMU in smartphone cannot implement coarse alignment by itself since its low performance.
In this manuscript, a parallel filtering method are proposed to estimate the proper orientation of the smartphone, as shown in Figure 5. In details, the up axis can be easily identified by accelerometer data. The essential problem lies in the direction of horizontal axis. Assuming the rest two axis points to four directions of the vehicle, i.e., right, forward, left and backward. There are four combinations considering right-hand rule, as shown if Figure 5. Four EKF with different smartphone orientations run in parallel. Each EKF has reduced states to decrease the calculation, i.e., attitude misalignment φ, velocity error δv^n and boresight misalignment α which has strong correlation with smartphone orientation. After a while of running, the proper EKF are selected in a discriminator by comparing their performance. The criterion could be innovation or residual of the filter. It is based on that EKF will diverge when filter is wrongly initialized. Finally, a full EKF inherits the states of the proper reduced EKF.

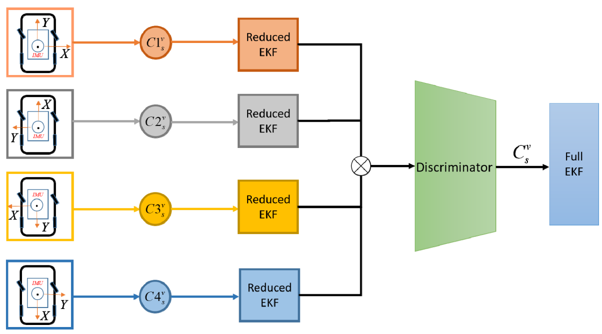

Figure 5. Reduced parallel filter

6. EXPERIMENTAL STUDY

6.1 Tunnel Experiment:

In the tunnel experiment the route starts from campus D of Chongqing University to campus A by the way of University Town tunnel, which get though Gele Mountain and has the length of 3555 meters. The GNSS signal was interrupted for 233 seconds in the tunnel. Huawei Mate20 phone was mounted in a more arbitrary attitude, as shown in Figure 6. Therefore, maneuver was made before entering the tunnel to converge the phone boresight misalignment and NHC level arm.

https://doi.org/10.5194/isprs-archives-XLVI-3-W1-2022-81-2022 | © Author(s) 2022. CC BY 4.0 License.

	Pitch misalignment (deg)	Roll misalignment (deg)	Heading misalignment (deg)	Right level arm (m)	Forward level arm (m)	Up level arm (m)	GNSS time lag （s）
Initial value	0	0	0	0	0	0	0
Calibration value	16.51	-62.97	118.1	-0.09	-2.49	-0.15	-1.26
Real value	N/A	N/A	N/A	-0.15	-2.55	-0.46	-1.15

Table 1. the calibration results in the tunnel experiment

Figure 7~11 show the calibration results of the, boresight misalignment, NHC lever arm, GNS time lag and vehicle trajectory, respectively. The boresight misalignment would converges to $\alpha = \left(16.51^{\circ} \quad -62.97^{\circ} \quad -118.1^{\circ}\right)$ after dynamic calibration (as shown in Table 1). It has obvious change between 1765s and 1827s because the vehicle was running at a turnaround and the boresight misalignment converges to the actual angle on the first round. This shows that continuous turning is necessary to estimate the boresight misalignment.

For the level arm, the right and up components changed slightly, while the forward component estimation of level arm had significant change when the vehicle was turning, as shown in Figure 8. The estimated level arm and their real values are listed in Table 1. The errors of right and forward level arm were only several centimetres, whereas the error of the up direction is five times than the right and forward. This is because the vehicle made a limited angular maneuver by the horizontal axis, which consequently resulted in a small level arm effect and weak observability.

Time synchronization is the prerequisite of integrated navigation. However, more than 1s time lag was observed between GNSS heading and INS heading, as shown in Figure 9. It is not appropriate to compensate time lag with a constant. In order to estimate the accurate bias, level arm and boresight misalignment, it is necessary to consider the time difference compensation. Therefore, GNSS time lag and BLE time lag are considered as synchronization error of EKF.As shown in the Figure 10, the GNSS time lag had been calibrated in the maneuver. According to the equation 9, The estimate of the GNSS time lag is affected by velocity. The GNSS time lag converges to -1.26s, which is close to time difference between GNSS and INS heading as shown in Figure 9.

The vehicle's trajectory is shown in Figure 11. The horizontal positioning error at the tunnel exit is 109.8m meters, which is 3.1% of mileage.

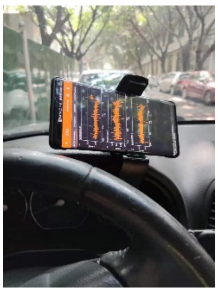

Figure 6. Smartphone mounting in tunnel experiment

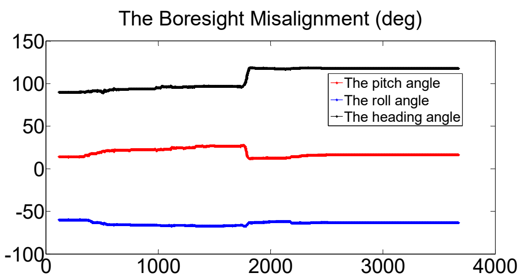

Figure 7. The boresight Misalignment in tunnel experiment.

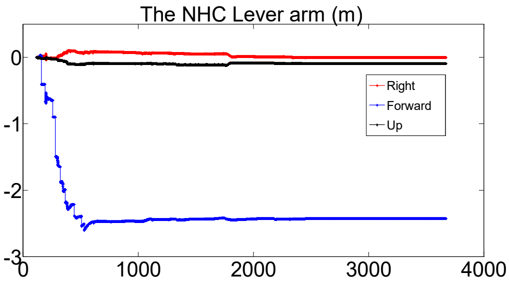

Figure 8. The NHC lever arm in real tunnel experiment (Red: the right lever arm; Blue: the forward lever arm; Black: the height lever arm)

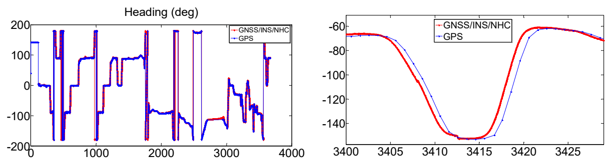

Figure 9. Heading of Vehicle in real tunnel experiment (left: GNSS and Integration heading; right: heading details)

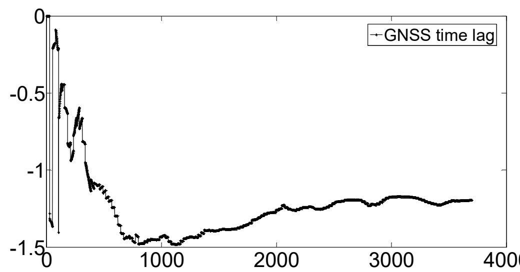

Figure 10. The GNSS time lag in real tunnel experiment

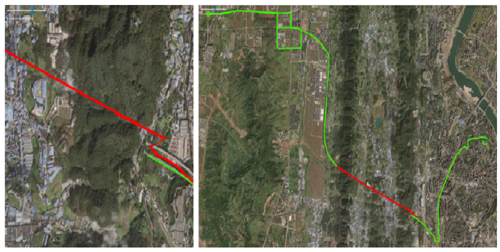

Figure 11. Vehicle trajectory in real tunnel experiment (Green : GNSS; Red: GNSS/INS/NHC integration)

6.2 Underground Parking Garage Experiment with BLE

In the underground parking garage experiment, BLE positioning infrastructure is available. Figure 12 depicts the layout diagram of BLE in underground parking garage. The base stations are 20m spaced out for positioning based on AOA principle. A Xiaomi K40 is used as shown in Figure 13. The vehicle run 152s with 16 turning and 798m mileage. Three positioning methods including BLE, INS/NHC and INS/NHC/BLE are used for comparison. BLE and integration trajectory coincide well with each other in most of time. However, un-smoothing was found in BLE route at the turning point. Similar phenomenon was also found in BLE heading, which even changes more than 40 degrees, as shown in the Figure 14. The trajectory of INS/NHC solution is smoothed, but it deviates from real route. The positional error reached tens of meters because many turnings and bump in the garage.

https://doi.org/10.5194/isprs-archives-XLVI-3-W1-2022-81-2022 | © Author(s) 2022. CC BY 4.0 License.

INS/NHC/BLE gets the best solution, the route is correct and well smoothed. Figure 15 describe the position innovation of INS/NHC/BLE EKF, i.e. positional difference between BLE and integration. Most of innovation is under 1 meter.

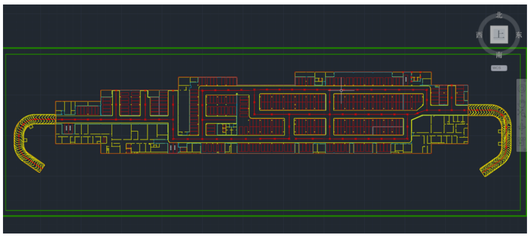

Figure 12. The layout diagram of BLE in underground parking garage (Red Dot: BLE base station)

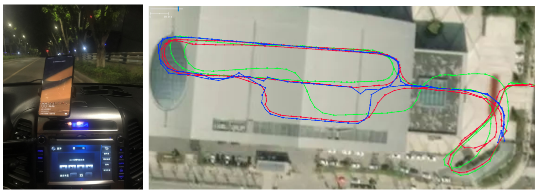

Figure 13. Smartphone mounting and the trajectory in underground parking garage (Blue: BLE; Green: INS/NHC; Red: INS/NHC/BLE)

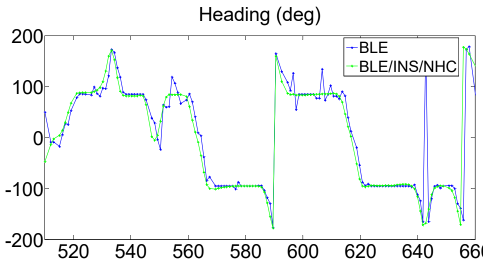

Figure 14. Heading in underground parking garage (Blue: BLE; Green: BLE/INS/NHC integration)

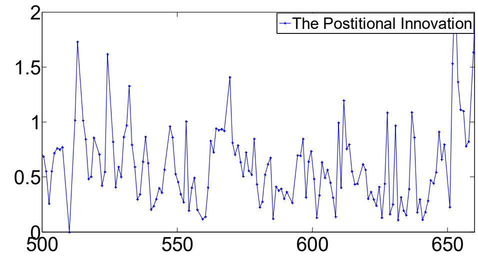

Figure 15. The Positional Innovation of BLE/INS/NHC integration in underground parking garage

7. CONCLUSION

Aims to promoting the application of smartphone-based vehicle navigation in full city scenarios, BLE/GNSS/INS integration plus Non-Holonomic Constraint was studied utilizing the phone built-in sensors. Some practical problems in smartphone navigation, such as arbitrary installation, NHC lever arm and time lag, are resolved by dynamic calibration and compensation. Two field tests were conducted in tunnel and underground parking garage, respectively. The experiment results verified that though cheap sensors are built in the smartphone, it can achieve surprisingly performance after delicate calibration. On the other hand, it indicate that the calibration of the boresign misalignment, the GNSS time lag and the NHC lever arm, would converge to a reasonable value after dynamic calibration.

ACKNOWLEDGEMENTS (OPTIONAL)

This research was funded by Open Research Fund of State Kay Laboratory of Information Engineering in Surveying, Mapping and Remote Sensing, Wuhan University (Grant No. 20P02).

REFERENCES

Cao, Z.P., Cheng, Y.F., Chen, R.Z., Guo, G.Y., Ye, F., Chen, L., Pan, Y.J., 2019: An infant monitoring system with the support of accurate real-time indoor positioning. *Geo-spatial Information Science*, 22(4): 279-289.

Chen, Q., Zhang, Q., Niu, X., 2021: Estimate the Pitch and Heading Mounting Angles of the IMU for Land Vehicular GNSS/INS Integrated System. *IEEE Transactions on Intelligent Transportation Systems*, 22:6503-6515.

Chen, R., Wang, L., Li, D., Chen, L., Fu, W., 2019: A Survey on the fusion of the navigation and the remote sensing techniques. *Acta Geodaetica et Cartographica Sinica*, 48:1507-1522.

Du, S., Zhang, S., Gan, X.D., 2022: A Hybrid Fusion Strategy for the Land Vehicle Navigation Using MEMS INS, Odometer and GNSS. *IEEE Access*, 8: 152512-152522.

Hiromune, N., Osamu, S., 2021: Indoor Location Estimation by Bluetooth Low Energy for Pedestrian Navigation. *IEEJ Journal of Industry Applications*, 10(1): 45-52.

Li, L.L., Sun, H. X., Yang, S., Ding, X.W., Wang, J., Jiang, J.L., Pu, X.H., Ren, C.H., Hu, N., Guo, Y.C., 2018: Online calibration and compensation of total odometer error in an integrated system. *MEASUREMENT: JOURNAL OF THE INTERNATIONAL MEASUREMENT CONFEDERATION*. 123:69-79.

Liu, C.Y., Ion., 2012: In 25th International Technical Meeting of the Satellite-Division of the Institute-of-Navigation, USA

Ning, Y, P., Sang, W.G., Yao, G.B., Bi, J.X., Wang, S.D., 2020: GNSS/MIMU tightly coupled integrated with improved multi-state ZUPT/DZUPT constraints for a Land vehicle in GNSS-denied environments. *International Journal of Image and Data Fusion*,12(3): 226-241.

Niu, Z., Nie, P., Tao, L., Sun, J.R., Zhu.B.C., 2018: RTK with the Assistance of an IMU-Based Pedestrian Navigation Algorithm for Smartphones. *Sensors*,19(14):3228.

Shin, E.H.,2005. Estimation techniques for low-cost inertial navigation. University of Calgary (Canada).

Wang, D. J., Dong, Y., Li, Z.Y., Li, Q.S., W, J., 2020: Constrained MEMS-Based GNSS/INS Tightly Coupled System With Robust Kalman Filter for Accurate Land Vehicular Navigation. *IEEE TRANSACTIONS ON INSTRUMENTATION AND MEASUREMENT* , 69(7): 5138-5148.

Zhang, Q., Hu, Y., Niu, X., 2020: Required Lever Arm Accuracy of Non-Holonomic Constraint for Land Vehicle

Navigation. *IEEE Transactions on Vehicular Technology*, 69:8305-8316, 69(8): 8305-8316.